


Features of Seasonal Variability of Chlorophyll *a* Concentration in Different Regions of the Southern Atlantic Based on Satellite Data

Ya. I. Bakueva , E. A. Kubryakova, A. A. Kubryakov

Marine Hydrophysical Institute of RAS, Sevastopol, Russian Federation

 *yasya1egupova@gmail.com*

Abstract

Purpose. Based on the long-term satellite optical measurements, the work is to study seasonal variability of the chlorophyll *a* concentration on the sea surface in different regions of the Southern Atlantic, determine its spatial features, identify the areas where the values of the chlorophyll *a* concentration are maximum, and to analyze the reasons for its increase in these regions.

Methods and Results. The data on the chlorophyll *a* concentration obtained from the MODIS-Aqua measurements for 2002–2019 in the region 30°–80°S, 70°W – 25°E were used. Spatial variability of the surface chlorophyll *a* concentration, its seasonal dynamics and the time of the seasonal peak occurrence were studied. Four zones of local maxima of the chlorophyll *a* concentration were identified (the Argentinean shelf, the islands of South Georgia, the area of water removal from the Antarctic Peninsula and the Antarctic shelf east of the Weddell Sea); for each of them the features of seasonal variability were analyzed in details.

Conclusions. In agreement with the previous papers, the peak chlorophyll *a* concentration and the beginning of bloom in the regions under study are observed later than in the high latitudes: in the northern part – in November – December, and in the southern one – in January – February. The exception consists in the quite extensive areas to the east of the nutrients powerful sources (islands, shelf waters), where the time of occurrence of the chlorophyll *a* concentration peak values is related to the advection impact, that results in its arising with a delay which is required for transferring the nutrients by the currents. The basic factors promoting appearance of the areas with the increased chlorophyll *a* concentrations are the interaction between the topography features and the Antarctic Circumpolar Current fronts, and ice melting in the marginal zone.

Keywords: Southern Atlantic, concentration of chlorophyll *a*, MODIS-Aqua, phytoplankton, seasonal variability, Antarctic shelf, satellite data, Weddell Sea, South Georgia Islands, Antarctic Peninsula, shelf

Acknowledgments: Analysis of seasonal variability of chlorophyll *a* concentration and data processing were supported by the Russian Science Foundation grant 21-77-10059, data processing was carried out within the framework of state assignment FNNN-2021-0003, and features of spatial variability of chlorophyll *a* concentration were studied within the framework of state assignment FNNN-2021-0010.

For citation: Bakueva, Ya.I., Kubryakova, E.A. and Kubryakov, A.A., 2023. Features of Seasonal Variability of Chlorophyll *a* Concentration in Different Regions of the Southern Atlantic Based on Satellite Data. *Physical Oceanography*, 30(1), pp. 27-46. doi:10.29039/1573-160X-2023-1-27-46

DOI: 10.29039/1573-160X-2023-1-27-46

© Ya. I. Bakueva, E. A. Kubryakova, A. A. Kubryakov, 2023

© Physical Oceanography, 2023

1. Introduction

The study of the Antarctic region bioproductivity is of great practical and fundamental interest due to its high bioresource potential. The Southern Ocean ecosystem is characterized by a number of unique features, the main ones are a large number of major nutrients (nitrates, phosphates) and a relatively low phytoplankton biomass [1, 2]. These features are believed to be due to a lack of



iron [3], a low level of irradiance in winter, frequent cloudiness, presence of ice [4, 5] and intense wind mixing, which leads to the formation of a deep mixed layer [6]. The concentration of iron and irradiance are the main limiting factors for the growth of phytoplankton cells [1, 2]. The main sources of iron in the region are terrigenous suspensions, which enter the ocean in large quantities near islands, in the marginal ice zone and in upwelling zones [2, 7, 8].

The intensive large-scale and eddy dynamics contributes to the redistribution of biogenic elements, leading to a significant spatial heterogeneity in the distribution of chlorophyll *a* (Chl-*a*) concentration [7, 8]. The most complete information on the spatial inhomogeneity of Chl-*a* in the surface layer was obtained from satellite optical measurements [4, 7–11]. This data made it possible for the first time to determine the features of the seasonal variability of the Chl-*a* concentration on the surface in various regions of the Antarctic [4, 7, 11].

In [11], based on satellite and *in-situ* data, the regional features of the seasonal variability of Chl-*a* bloom in different zones of the Drake Strait was carried out, and the relationship between the seasonal variability of Chl-*a* including cooling and irradiance was discussed. A shift of peak Chl-*a* concentration values from November to January from north to south was observed. In [4, 7], a significant variability in the distribution of Chl-*a* concentration in highly productive zones and oceanic deserts was demonstrated. For the first time, based on these data, it was demonstrated that the highest productivity zones are tied to topographic features, from which they extend thousands of kilometers under the influence of advection [7, 8]. The authors of [8] attribute the Chl-*a* concentration increase to upwelling that occurs when topographic irregularities affect the water flow. Large Chl-*a* concentrations, according to various data, are observed during the period of ice melting in the Antarctic [12], the distribution of these marginal blooms also has a strong spatial variability [13, 14].

One of the most important and most productive regions of the Antarctic is the southern part of the Atlantic Ocean [4], which is currently the focus of expeditionary research in Russia [9, 11, 15–19]. It is characterized by the sharpest variability of hydrodynamic and hydrobiological processes associated with a number of features: the intensification of the Antarctic Circumpolar Current (ACC) in the Drake Strait area, the collision of the Brazil and Falkland currents, the presence of a number of islands that are a source of terrigenous nutrients, as well as the Antarctic Peninsula protruding into the open ocean. Intensive dynamics significantly affects the ecosystem functioning in this region. Its important characteristic is Chl-*a*, which is an indicator of phytoplankton biomass. It is the phytoplankton biomass distribution that largely determines the spatial variability of its consumer, zooplankton, including the economically important – krill. Understanding the features of the seasonal variability of chlorophyll *a* concentration in different regions is necessary in the preparation and analysis of the data from Russian Antarctic expeditions.

Based on the long-term satellite optical measurements from 2002 to 2019, the present paper is aimed to study seasonal variability of the Chl-*a* concentration on the sea surface in different regions of the Southern Atlantic, to determine its spatial features, to identify the areas where the values of the Chl-*a* concentration are maximum, and to analyze the reasons for its increase in these regions. This

article uses materials from the report presented at *The Seas of Russia: Challenges of the National Science All-Russian Scientific Conference* ¹.

2. Data and methods

For the study, the surface Chl-a concentration data obtained from the MODIS-Aqua satellite scanner data for 2002–2019 in the South Atlantic in the region of 30°–80°S, 70°W–25°E were used. The Level 3 data were downloaded from <http://oceancolor.gsfc.nasa.gov/>. The Chl-a concentration was calculated according to the standard method using the *OC3M* algorithm for MODIS and *OC4* for SeaWiFS [20]. The spatial resolution of the data used is 4 km.

We shall note that satellite methods for Chl-a concentration simulation give an error and its average estimate is about 30% [20]. According to [21], the standard NASA *OC4* 4 algorithm leads to an underestimation of Chl-a concentration in the Atlantic sector of the Southern Ocean by more than 0.2 mg/m³. The developed regional algorithms lead to a slight decrease in the standard deviation by 0.1 mg/m³ [22]. However, for example, in [9], based on a comparison of satellite and expeditionary data in the South Atlantic, it was shown that the correlation coefficient between these data exceeded 0.93, and it was concluded that they can be used to estimate the Chl-a content in the surface layer in the Antarctica areas under consideration. The present paper is mainly devoted to a qualitative description of the spatial and temporal variability of Chl-a concentration, as well as to the determination of areas of maximum Chl-a concentration on the sea surface. When interpreting the results, it is necessary to take into account the inevitable inaccuracies in the described absolute values of Chl-a concentration associated with the satellite data application.

3. Seasonal Chl-a concentration variability

The average spatial distribution of Chl-a concentration on the sea surface for 2002–2019 for the considered region (Fig. 1) demonstrates a significant spatial heterogeneity of its values. The zones of high concentrations with values of 0.5–1 mg/m³ are concentrated mainly to the east of the Drake Strait, while Chl-a concentration in the strait itself are much lower (0.1–0.2 mg/m³). Fig. 1 shows several regions where the average Chl-a concentration values according to satellite data reach rather high numbers – over 1 mg/m³:

- region 1 – the east coast of South America, south of La Plata Bay, which the second largest river in South America, the Parana, flows into. From here, the waters with high Chl-a concentration are transported eastward along the subantarctic front;
- region 2 – the area of deep-water outflow by the polar front near the South Georgia Islands;
- region 3 – the area of water removal from the marginal zone of the Antarctic Peninsula;
- region 4 – the Antarctic shelf east of the Weddell Sea.

¹ Bakueva, Ya.I., Kubryakova, E.A. and Kubryakov, A.A., 2022. Features of Seasonal Variability in Chlorophyll a Concentration in the Atlantic Sector of the Southern Ocean from Satellite Data. In: MHI, 2022. *The Seas of Russia: Challenges of the National Science. Proceedings. September 30, 2022, Sevastopol*. Sevastopol: FSBSI FRC MHI, pp. 180-181 (in Russian).

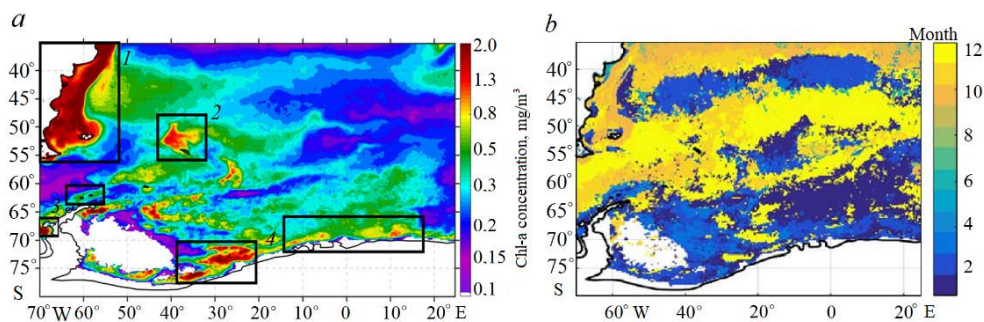


Fig. 1. Average spatial distribution of the Chl-a concentration (mg/m^3) (a) and maximum Chl-a concentration by months (b) based on the MODIS-Aqua satellite observations in the area under study for 2002–2019

Further, a detailed analysis of the Chl-a concentration variability for each of these individual regions will be carried out.

Between regions 1 and 3, there is a zone of low Chl-a concentration associated with advection of poor Pacific waters through the Drake Strait. The tongue of these waters changes its position depending on the season and from year to year. In Fig. 1, a, it is observed up to 40°W , i.e., up to region 2 – the South Georgia Islands.

The diagram of the average seasonal variability of Chl-a concentration (Fig. 1, a) for the considered area at each latitude shows that in its northern part, above 45°S , the satellite data on Chl-a concentration is obtained all year round. South of 45°S , the diagram shows a fairly large zone where the data is completely absent due to the polar night; therefore, it is not possible to study the Chl-a concentration variability from satellite data for the entire year in this region.

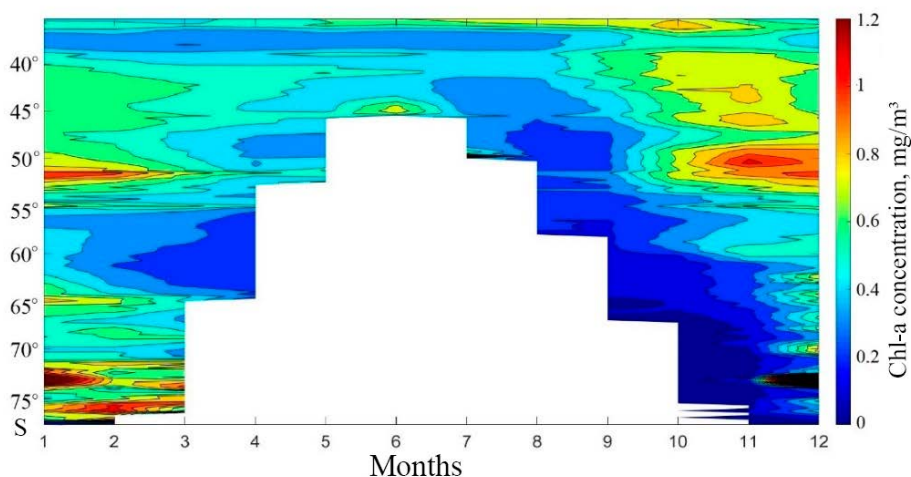


Fig. 2. Seasonal diagram of the longitudes averaged Chl-a concentration variability at different latitudes for the area under study for 2002–2019

The diagram (Fig. 2) clearly shows a pronounced feature – with increasing latitude, the Chl-a concentration peak and the beginning of blooming are observed later. This feature, noted in [4, 9], is associated with different periods of intense heating and the appearance of stable thermal stratification, which causes the blooming to start.

Chl-a concentration in the northern part of the study area (35°–45°S) starts to increase, as a rule, from September to October annually, reaching a maximum of average values by November. The above average values are observed from September to April. At 35°–45°S latitudes, a similar pattern of seasonal dynamics of Chl-a concentration is observed. The areas with a minimum Chl-a concentration (about 0.2 mg/m³) were recorded from August to September, the areas with a maximum Chl-a concentration were recorded from November to February with local maxima within 0.9–1.1 mg/m³. Some latitudes are distinguished by very high Chl-a concentration, which is associated with the location of certain topographic features here, such as: islands and shelf zones, which are discussed in more detail in the next section.

At 55°–65°S latitudes the smallest amplitudes of the seasonal variability of Chl-a concentration are observed. The minimum is observed from August to April, and the increased values – from October to February. In these latitudes, there is the Drake Strait, as well as deep-sea regions of the South Atlantic, where the Chl-a concentration values are minimal.

From 65°S to 75°S, the blooming, as a rule, is observed from November, reaching a maximum in December – January (values more than 1.2 mg/m³) and continuing until March. In these areas, satellite observations enable us to have data from two to four months a year, depending on the latitude. This observation area is located in the southern part of the area near the Antarctic shelf. Presumably, the Chl-a concentration increase here is associated with the marginal ice melting.

To determine the spatial variability of the time to reach the peak Chl-a concentration values, its seasonal variation was calculated at each point of the array. Next, the month corresponding to its maximum was determined (see Fig. 1, *b*). The time to reach peak Chl-a concentrations varies from October to March in different areas. The earliest peak is recorded in October – November: in the warmest waters over the Patagonian shelf, in subtropical latitudes (above 40°S). At the same time, a peak is recorded in the southern part of the Drake Strait. The reason for the Chl-a concentration increase to peak values in this area is the presence of sources of nutrients in the shallow areas of the South Shetland Islands shelf. By December, the peak values shift to the central parts of the area at 45°S latitude. In January and February, the maximum increase in Chl-a concentration is recorded in the southern part of the Atlantic sector, mainly south of 65°S, up to the Antarctic shelf. At the same time, in January, the peak is recorded only in the seaward eastern part of the Weddell Sea and in the Scotia Sea, which are ice-free at this period.

On the map of average monthly maximum Chl-a concentrations (see Fig. 1, *b*), there are two areas in the north where the peak is also observed in January – February: 1) on the boundary of the Polar and Subantarctic fronts, between 40° and 48°S; 2) the area east of the South Georgia Islands (10°–20° E, 50°–60° N). The reason for this peak shift in both areas is probably the horizontal advection of Chl-a and nutrients from the areas of their high concentration. In the first case,

the source of nutrients is the Argentine shelf waters, in the second – the South Georgia Islands (see Fig. 1, *a*). These processes will be discussed in more detail below.

An analysis of seasonal maps (Fig. 3) shows that the Chl-*a* concentration increase begins in September near the South America coast in the area where the Falkland and Brazil currents meet. In September, an area with a high Chl-*a* concentration is observed on the entire Argentinian shelf around the southern coast of the Tierra del Fuego archipelago and up to the Falkland Islands (from 0.7 to more than 2.0 mg/m³). This is most likely due to the Parana River runoff intensification in spring and its entry into the shelf zone under the influence of the Brazil Current advection in this area.

In October, the areas with high Chl-*a* concentration (over 2.0 mg/m³) spread over the entire Argentinean shelf and reach the extreme point of the Tierra del Fuego archipelago – Cape Horn in the south and the Falkland Islands in the east. The subsequent increase in Chl-*a* concentration falls on the late Antarctic spring: mid-late November. At this time, there is a widespread increase in the zones with elevated Chl-*a* concentrations and the appearance of an area of high concentrations at the southern boundary of the Polar Front near the South Georgia Islands (50°–60°S, 30°–50°W). The sharp increase in Chl-*a* concentration in these areas is associated [7, 8] primarily with the removal of terrigenous suspension and nutrients from the islands and the shelf surrounding them. In addition, the upwelling probably plays an important role. It is caused by a shift in the ACC velocity when flowing around the shelf of islands, leading to a sharp rise in nutrients from deep layers [8].

The bands of high Chl-*a* concentrations from the South Georgia Islands extend far to the east up to 10°E longitude. Such band expansion is associated with the spread of nutrients from the islands under the action of ACC advection [8]. The South Georgia Island in this case acts as a permanent source of nutrients, which continuously supplies nutrients to the area to the east of it. By December, the band of high Chl-*a* concentrations extends ~ 5000 km to the east. Indeed, according to the altimetry data, the ACC velocity is about 0.5 m/s, then it will shift by ~ 4000 km in three months. This shift explains the blooming peak shift in region 2 (35°–45°E, 50°–60°S) (Fig. 3). In the northern part of the area under study, the region of high values associated with another source (the Parana River) also extends significantly to the east, reaching 10°W and causing a shift in the blooming peak in this zone.

From the beginning of December, the zones with elevated Chl-*a* concentrations shift to more southern latitudes, up to the continental shelf edge east of the Antarctic Peninsula, and by the end of December they spread along the Antarctic shelf. In this area, the Chl-*a* concentration dynamics in January is most pronounced, when high values reach more than 0.6 mg/m³ and are concentrated on the Antarctic shelf edge. Here they are observed until February, in March the Chl-*a* concentration decreases significantly.

Then, a rather dynamic, widespread decrease in Chl-*a* concentration to 0.1–0.5 mg/m³ begins by early April, except for the area near the Parana and Uruguay rivers (Fig. 3, *g*, *h*). It should be noted that the Chl-*a* concentration data from April

to October are unavailable due to the optical features of the scanner and ice formation (Fig. 3, $k - n$).

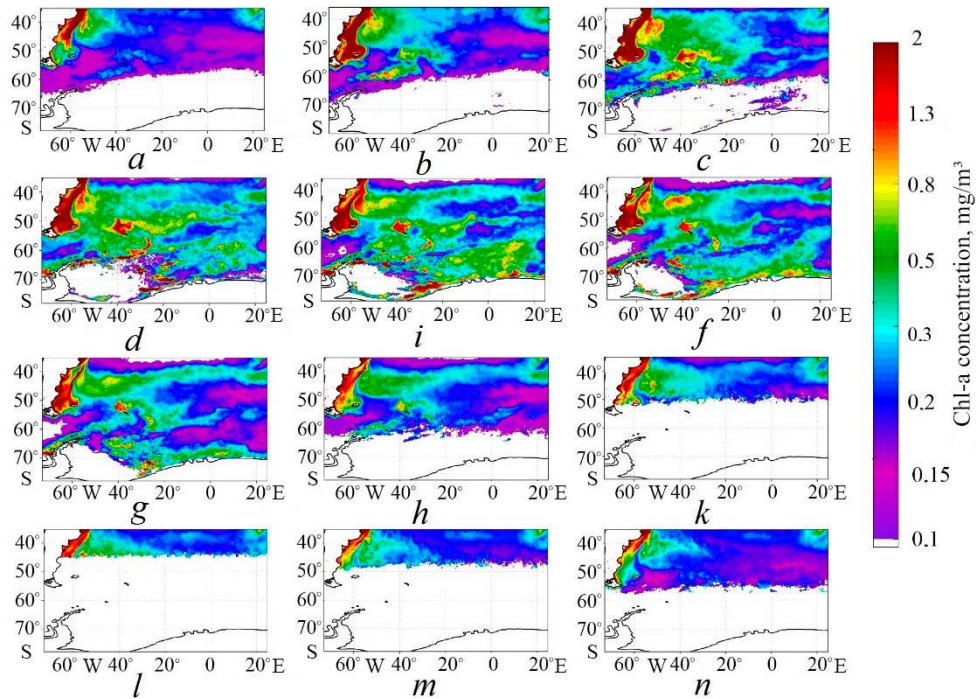


Fig. 3. Average Chl-a content in the selected region (30° – 80° S, 70° W– 25° E) based on the MODIS-Aqua satellite observations in September (*a*), October (*b*), November (*c*), December (*d*), January (*e*), February (*f*), March (*g*), April (*h*), May (*k*), June (*l*), July (*m*) and August (*n*) for 2002–2019

The Drake Strait should be singled out as a separate region, which is distinguished by the lowest Chl-a concentrations [7, 8], associated with the advection of biologically-poor Pacific waters through the strait. In the western part of the strait, a low Chl-a concentration (less than 0.2 mg/m^3) is observed in all seasons. In the eastern part, in November – December, there is a seasonal peak in the Chl-a concentration growth to values of 0.3 – 0.5 mg/m^3 , associated with the spread of nutrients from the areas of the southern boundary of the Polar Front. The position and intensity of the inflow of Pacific waters and the minimum of Chl-a concentration have a pronounced seasonal and interannual variability, which significantly affects the spatial distribution of Chl-a concentration in this area.

4. Regional features of Chl-a concentration variability in its local maxima zones in the South Atlantic

For a more detailed understanding of the physical factors of the Chl-a concentration increase, a detailed study of its variability in four selected regions was carried out (see Fig. 1).

4.1. Region 1 – the Argentinean shelf

The region of the east coast of South America is located south of La Plata Bay, between 22° – 59° S and 46° – 75° W. This area is characterized by high Chl-a

concentrations throughout the year, which is associated with the outflow of river waters from the Parana and Uruguay rivers (the annual flow of rivers into the ocean is 650 km³ in total). The main feature of spatial variability is the area with Chl-a concentrations over 1.3 mg/m³, which coincides with the position of the Argentinean shelf. In August, such waters are observed to 100 m depth, in September – to 200 m and in October – to 500 m depth.

The Chl-a concentration decrease in this region, which is especially pronounced in the shelf center, is observed in summer. In June, its high values are localized in the coastal part of the area near the Parana River mouth, as well as on the Argentinean shelf edge at depths of 100–200 m (Fig. 4, *a*). The same distribution of concentrations is observed during July and August, when high values occupy even smaller areas (Fig. 4, *b*, *c*).

In September, the Chl-a concentration in these areas begins to grow, especially in the northern part of the area, from where rich in Chl-a waters are carried along by the Brazil Current and mesoscale eddies to the southeast (Fig. 4, *d*).

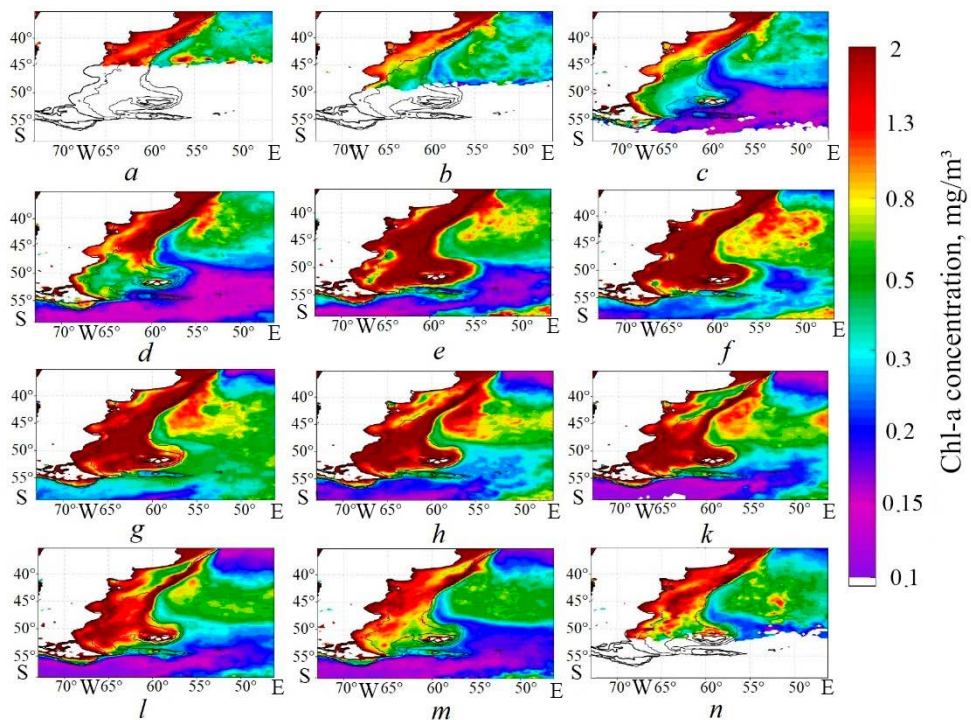


Fig. 4. Distribution of the monthly-averaged Chl-a concentration in June (*a*), July (*b*), August (*c*), September (*d*), October (*e*), November (*f*), December (*g*), January (*h*), February (*k*), March (*l*), April (*m*) and May (*n*) in 2002–2019. The 100, 200 and 500 m isobaths are plotted on the maps

By October (Fig. 4, *e*), the Chl-a concentrations reach their maximum (more than 5 mg/m³) and occupy almost the entire Argentinean shelf to a depth of 500 m, reaching the Falkland Islands. From October to December, its values increase in the southern part of the region and decrease in the northern. The Chl-a concentration distribution is very uneven in space. Climate maps show a number of

local maxima and minima, which are probably associated with hydrological features – pronounced frontal zones in the area of conjugation of the Brazil and Falkland currents.

In the northern part of the region, there is a zone of transport of the waters rich in Chl-*a* to the east. The width increases with the beginning of the Antarctic summer (Fig. 4, *f* – *k*), then it shifts south by February. Further, the areas of distribution of Chl-*a* rich waters narrow to the east, forming a rather narrow alluvial corridor by April (Fig. 4, *m*). A powerful local blooming in May is noted over the deep-water part of the area in the eastern part of the region. Further development of this blooming cannot be observed in June and July due to the lack of data at these latitudes (Fig. 4, *a*, *b*).

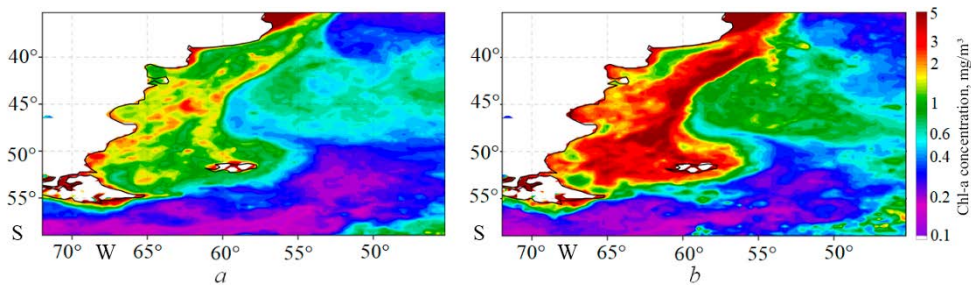


Fig. 5. Distribution of the annual-averaged Chl-*a* concentrations in the selected region for 2005 (*a*) and 2011 (*b*)

The Chl-*a* concentration variability is characterized by pronounced interannual fluctuations affecting the entire study area. Fig. 5 shows maps of average annual Chl-*a* concentrations on the surface according to the satellite observations for 2005 and 2011. In 2005, the average annual value of Chl-*a* concentration was minimal, and the areas with high values occupied the smallest areas. In 2011 (Fig. 5, *b*), a peak of Chl-*a* concentration was recorded in this area for 2002–2019. At that time, the concentrations on the entire Patagonian shelf and in the northeastern part of the area were twice as high as in 2005.

4.2. Region 2 – South Georgia Islands

The next region under consideration is located near the South Georgia Islands between 48°–56°S and 32°–45°W. It is elongated in the latitudinal direction (see Fig. 1, *a*), which is associated with the transport of nutrients to the east of the ACC. It should be noted that, in this region, the satellite observation data on the Chl-*a* concentration is available almost all year round from August to April.

An analysis of the distribution maps of average monthly Chl-*a* concentrations enabled to specify the spatial and temporal characteristics of blooming in this region using an example of monthly average maps for 2002–2019. The 100, 200 and 500 m isobaths were plotted on the maps to better determine the boundaries of the increased Chl-*a* concentration areas.

The graph of temporal and seasonal variability (Fig. 6, *a*) shows that an annual sharp increase in the Chl-*a* concentration in this region has been observed on average since September, and the values reach their maximum in December (about

0.87 mg/m³ on average). Such high mean Chl-a concentrations do not last long, by January the values fall below 0.7 mg/m³. In general, from January to August, there is a noticeable decrease in concentrations (the minimum in August – about 0.2 mg/m³).

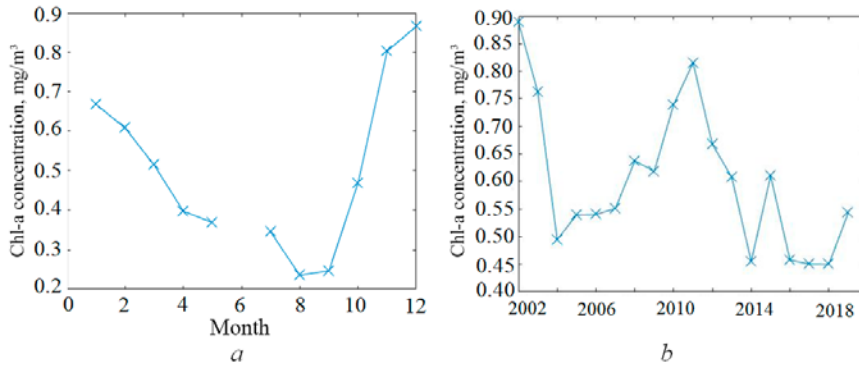


Fig. 6. Variability of the Chl-a average concentration in the region under study in 2002–2019: a) seasonal and b) annual average ones

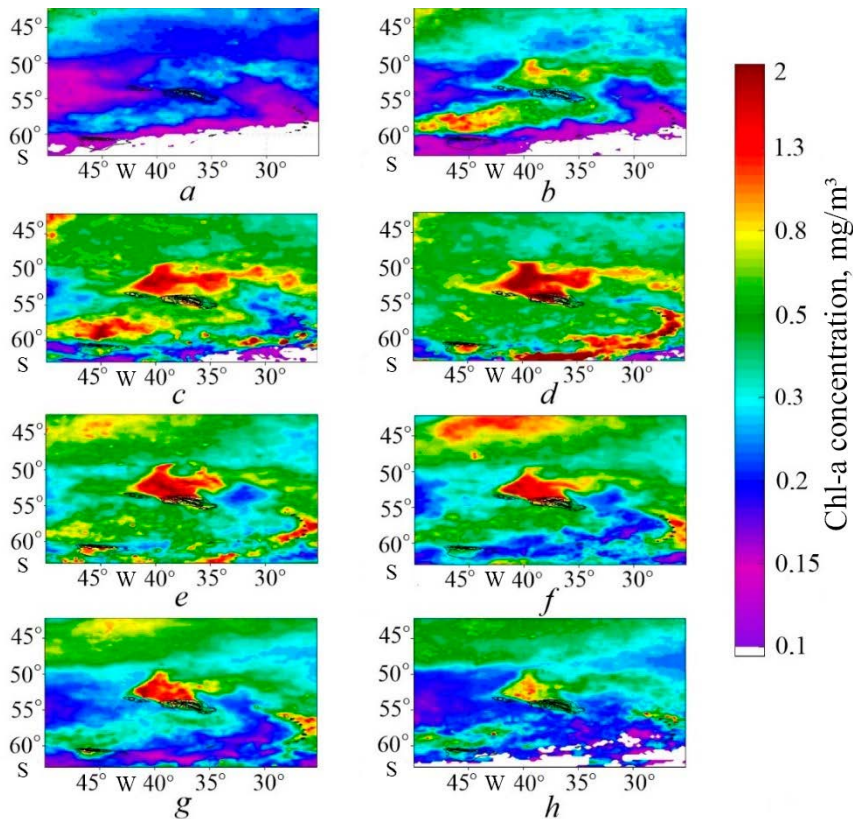


Fig. 7. Distribution of the monthly-averaged Chl-a concentrations in September (a), October (b), November (c), December (d), January (e), February (f), March (g), and April (h). The 100, 200 and 500 m isobaths are plotted on the maps

The analysis of average monthly maps made it possible to study in detail the spatial and temporal variability of the parameter under study. Some insignificant local increases in Chl-a concentration begin annually in September and have a pronounced meridional direction (Fig. 7, *a*), related to the transfer of nutrients and phytoplankton by the ACC flow. This is followed by a sharp increase in concentration in October, with high concentration zones located on the leeward side of shallow water banks at depths over 500 m. The maximum Chl-a concentrations are recorded in the eastern part of shallow banks, while the Chl-a-rich water outflow spread from west to east, reaching 25°W in November. The region of the maximum has a rhomboid shape in the area of 33°–43°W, 49°–55°S and is characterized by concentrations over 2 mg/m³.

This feature is most pronounced in December and January (Fig. 7, *d, e*), when such a blooming zone location demonstrates how significant the effect of topography features is on the ACC and, as a result, on the Chl-a concentration variability. The flow on the banks leads to the development of mesoscale eddies and upwelling, which may be one of the additional reasons for the nutrients flow increase in this area [23]. From February to April, the areas of high and average Chl-a concentration gradually decrease and shift to lower latitudes.

It should be noted that there is a powerful blooming observed south of the South Georgia Islands, which is especially pronounced in December. The blooming area is located in the marginal ice zone in the north of the Weddell Sea, and its location is apparently associated with the removal of nutrients during ice melting (Fig. 7, *d*).

From 2002 to 2019, in this region, the distribution of the average Chl-a concentration over the surface is uneven; throughout the season, both areas with high values and areas with stably low values are observed. The average Chl-a concentration is 0.55 mg/m³ (with the maximum and minimum values of the indicator reaching 3.64 mg/m³ and 0.13 mg/m³, respectively). Fig. 6, *b* shows a graph of the average annual Chl-a variability in the selected period, which clearly shows noticeable differences in concentration rates in different years. An example in Fig. 8 shows the average annual Chl-a concentration distribution in 2011 and 2016. In 2016 (Fig. 8, *b*), its average annual value was minimal, and the areas with high values occupied the smallest areas. In 2011 (Fig. 8, *a*), the Chl-a concentration peak was recorded in this area for 2002–2019. At this time, the average concentrations in the selected area increased twofold compared to 2016.

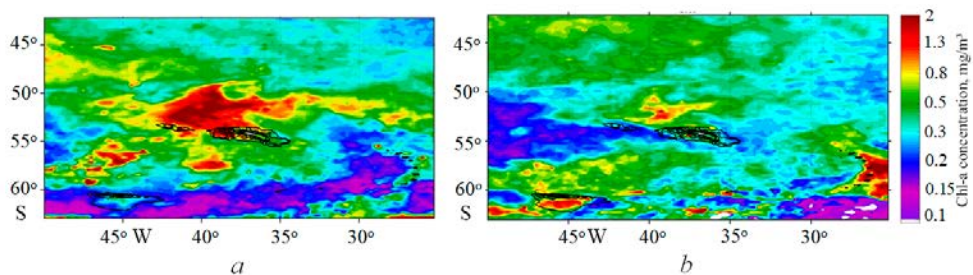


Fig. 8. Distribution of the annual-averaged Chl-a concentrations in the selected region for 2011 (*a*) and 2016 (*b*)

4.3. Region 3 – the Antarctic Peninsula shelf zone

Based on the spatial variability analysis, two main areas of blooming near the Antarctic Peninsula between 52° – 75° S and 65° – 72° W are distinguished (Fig. 9). The area *a* has a rectangular shape, is located in the western coastal part of the Antarctic Peninsula in the northern part of the Bellingshausen Sea within 64° – 67° S and 65° – 70° W, the area *b* is located near the South Shetland Islands within 61° – 64° S and 54° – 63° W. Both areas under study are located above the continental shelf with depths up to 500 m.

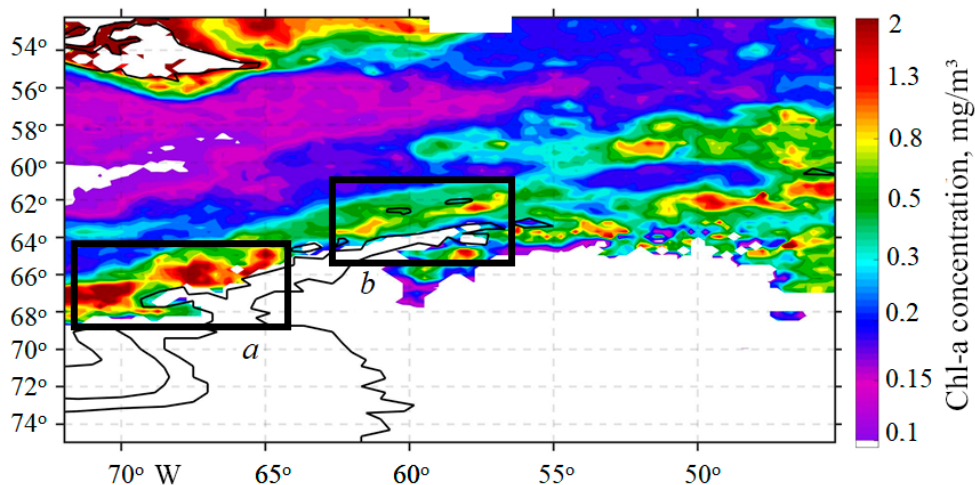


Fig. 9. Areas of the increased Chl-a concentrations near the Antarctic Peninsula based on the MODIS-Aqua satellite observations

Seasonal variability in both areas is similar (Fig. 10). From September to December, the concentrations increase, but in area *a*, the figures are much higher (0.55 mg/m^3 in area *a* versus 0.35 mg/m^3 in area *b*). An interesting observation: in area *a*, the Chl-a concentration also increases annually from March to April. From May to August, there are no data on Chl-a concentration in both regions.

The seasonal evolution of Chl-a concentration (Fig. 11) indicates an annual local increase in concentration starting from October, near the George VI shelf. This increase by November propagates along the southern front of the ACC near the Antarctic Peninsula shelf and is most likely associated with the removal of terrigenous nutrients from the marginal ice, as well as with the upwelling at the ACC front (Fig. 11, *a*). From December to March (Fig. 11, *c* – *f*), in area *a* region, the zone of the most intensive blooming (more than 2 mg/m^3) is localized. One of the important reasons for this process is marginal blooming, which occurs as a result of the ingress of nutrients into the water during ice melting. As a result of this process, as well as the removal of rich waters by the southern front of the ACC, the zone of high Chl-a concentrations spreads rather evenly along the entire continental shelf of the Antarctic Peninsula (Fig. 11, *d* – *f*), taking on the outlines of currents, after which it is carried out to the eastern part of the basin under the ACC influence.

As the blooming area in the marginal ice zone decreases (area *a*), the tongue of nutrient water removal to more northern latitudes also decreases (area *b*). This phenomenon is quite clearly seen in March (Fig. 11, *f*), when high Chl-*a* concentrations are observed only near the southwestern side of the Antarctic Peninsula. Starting from April, further distribution of blooming cannot be determined from optical data due to the lack of it (Fig. 11, *g, h*).

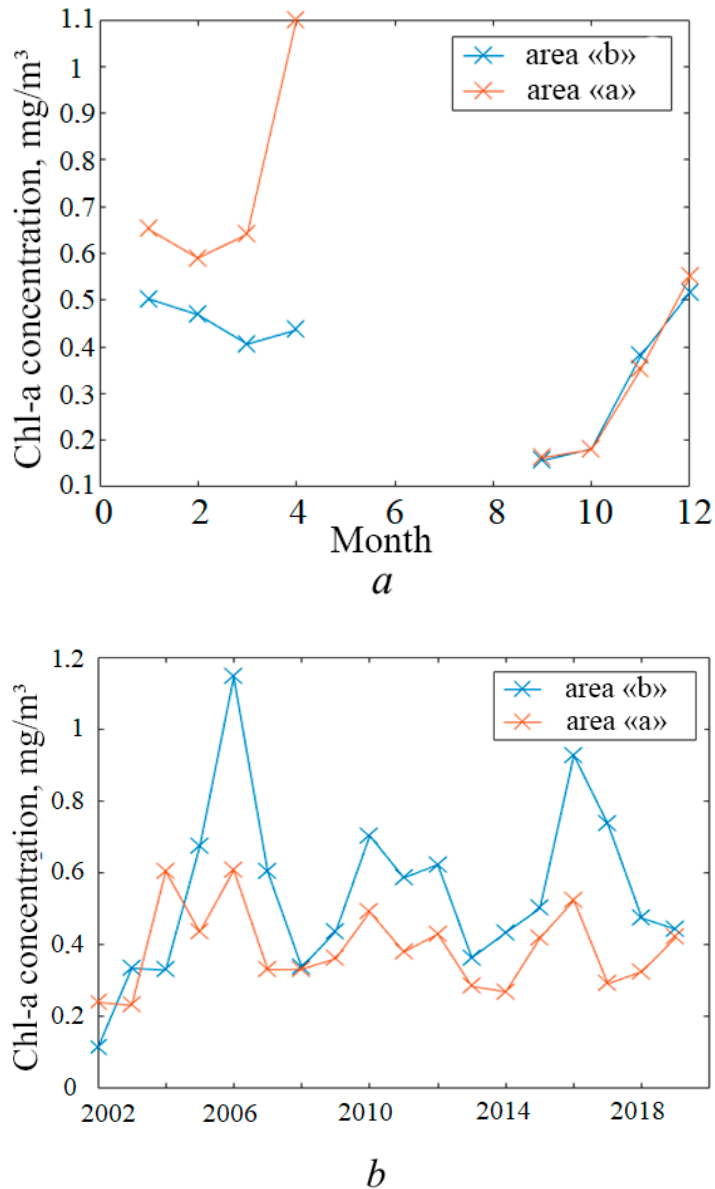


Fig. 10. Variability of the Chl-*a* average concentration in the region under study in 2002–2019: *a*) seasonal and *b*) annual average ones

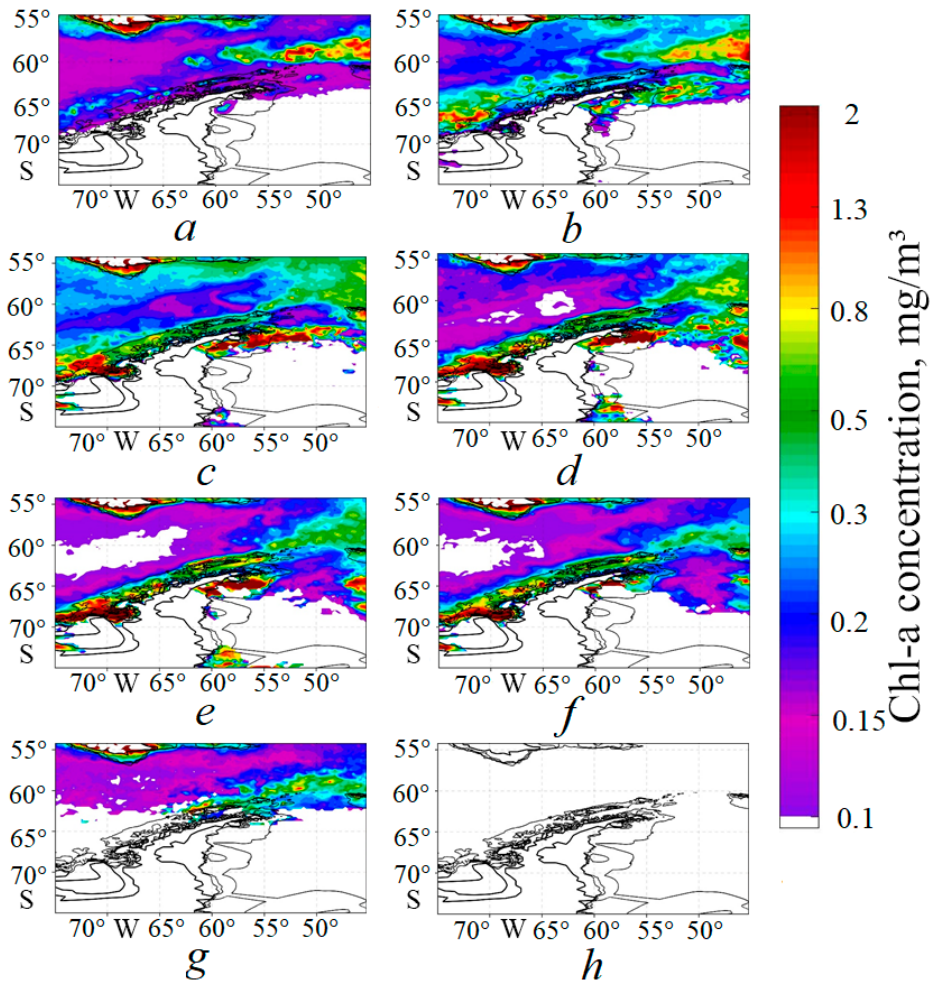


Fig. 11. Monthly-averaged distribution of the Chl-a concentrations in the selected area in October (a), November (b), December (c), January (d), February (e), March (f), April (g) and May (h) from 2002–2019 based on satellite observations. The 100, 200 and 500 m isobaths are plotted on the maps

As the blooming area in the marginal ice zone decreases (area a), the tongue of nutrient water removal to more northern latitudes also decreases (area b). This phenomenon is quite clearly seen in March (Fig. 11, f), when high Chl-a concentrations are observed only near the southwestern side of the Antarctic Peninsula. Starting from April, further distribution of blooming cannot be determined from optical data due to the lack of it (Fig. 11, g, h).

4.4. Region 4 – Antarctic shelf east of the Weddell Sea

The last distinguished region is localized in the region of southern latitudes: the Antarctic shelf and the southeastern part of the Weddell Sea between 66°–78°S and 10°– 50°W. This area is of interest because of the processes that cause an increase in Chl-a concentrations during ice melting. Blooming variability is determined not only by the surface layer heating, but also by the dynamics of the ice field boundary retreat with the effect of blooming on the edge of melting

ice, since from melting of ice, as well as from shelf deposits, a sufficient amount of iron enters the water.

This area is quite elongated in the latitudinal direction and has two epicenters of elevated Chl-a concentrations that differ from each other in space and time. In this regard, the entire area was also divided into two smaller areas: area *a* is square and is located in the southeastern part of the Weddell Sea within 71°–77°S and 20°–40°W, area *b* is elongated along the Antarctic shelf and is located between 66°–70°S and 10°–20°E (Fig. 12).

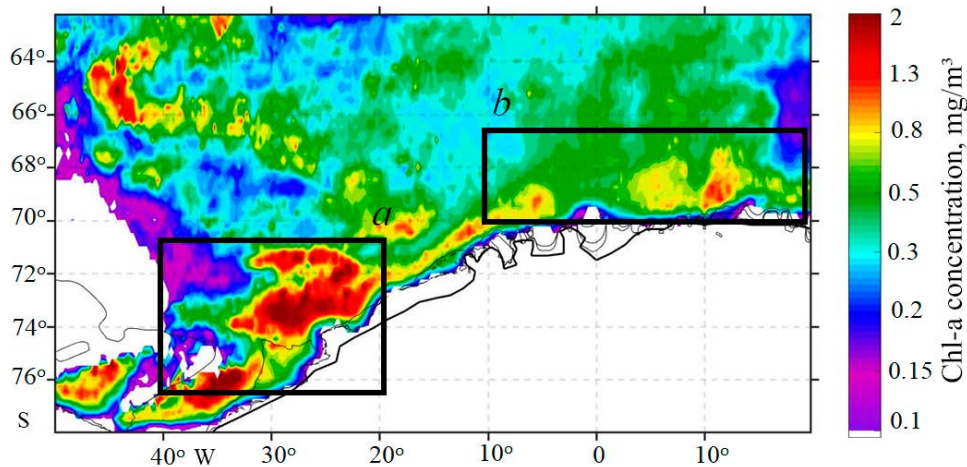
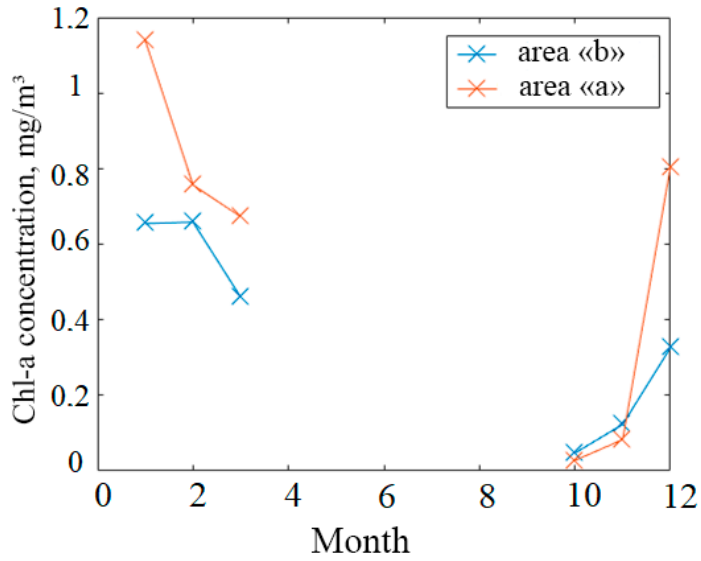
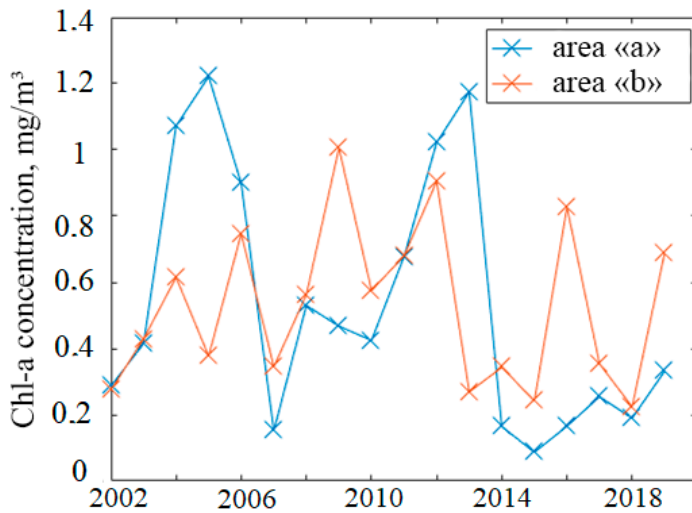


Fig. 12. Areas of the increased Chl-a concentrations in region 4 for 2002–2019 based on the MODIS-Aqua satellite observations

Despite the proximity of areas *a* and *b*, the average annual variability of Chl-a concentrations in this region is different. Thus, in area *a*, its average concentration for the entire time is 0.39 mg/m^3 , the maximum and minimum concentrations reach 4.14 mg/m^3 and 0.015 mg/m^3 , respectively. In area *b*, its mean concentration is 0.34 mg/m^3 , the maximum – reaches much lower values and is 2.07 mg/m^3 , the minimum one is 0.017 mg/m^3 . Fig. 13 shows the mean Chl-a concentration in two areas in different years. On the graph (Fig. 13, *b*), peaks of Chl-a concentrations varying by years can be seen. For area *a*, two large concentration peaks are observed (more than 0.9 mg/m^3 in 2004–2006 and 2012–2013), in other years the values do not exceed 0.6 mg/m^3 . Area *b* is characterized by a greater interannual variability of Chl-a concentrations, when peaks were observed every 1–2 years, but reached lower values than in area *a*. It should also be noted that there is no pronounced correlation between the indicators in the areas: the peak years for area *a* do not coincide with the peak years for area *b*, and vice versa. This indicates different physical factors affecting the increase in Chl-a concentration in these areas, in particular, differences in the ice cover.



a



b

Fig. 13. Temporal variability of the average Chl-*a* concentration in the regions under study in 2002–2019: *a*) seasonal and *b*) annual average ones

Based on the seasonal variability graphs, Chl-*a* concentrations are characterized by an annual increase starting from October. Blooming, as a rule, has maxima in January (for area *a*, the mean monthly figures reach 1.17 mg/m³, for area *b*, it is much lower – 0.65 mg/m³). After January, the concentrations drop sharply, reaching the observed lows in March. As mentioned above, from April to September, the data on the chlorophyll *a* concentration variability on the surface is absent.

The seasonal evolution of the Chl-a concentration distribution is described based on monthly average maps for 2002–2019. The 100, 200 and 500 m isobaths are plotted on the maps for better determination of the boundaries of areas of increased Chl-a concentrations. The extremely short annual observation period from November to March, which is related to the optical properties of satellite observations, bears mentioning.

During the analysis, an annual increase in the values of the indicator in December was noted, in most years starting at the boundary of the Weddell and Lazarev seas (Fig. 14, *a*). The waters with a high Chl-a content are carried from north to south and reach the continental shelf under the Weddell Cycle influence, which is clearly seen in Fig. 14, *b*, *c*. In general, the blooming develops from east to west along the marginal ice zone and by January forms areas of very high Chl-a values (with values sometimes exceeding 2 mg/m^3) in the southern Weddell Sea (Fig. 14, *b*), near the Ronne glacier and most of the Riiser-Larsen Sea area. These high values persist until February (Fig. 14, *c*). In March, the data on the Chl-a concentration on the sea surface in the western part of area *a* in most cases are not on the maps due to ice conditions, while in area *b* the concentration is characterized by a sharp decrease in values from very high to medium (Fig. 14, *d*).

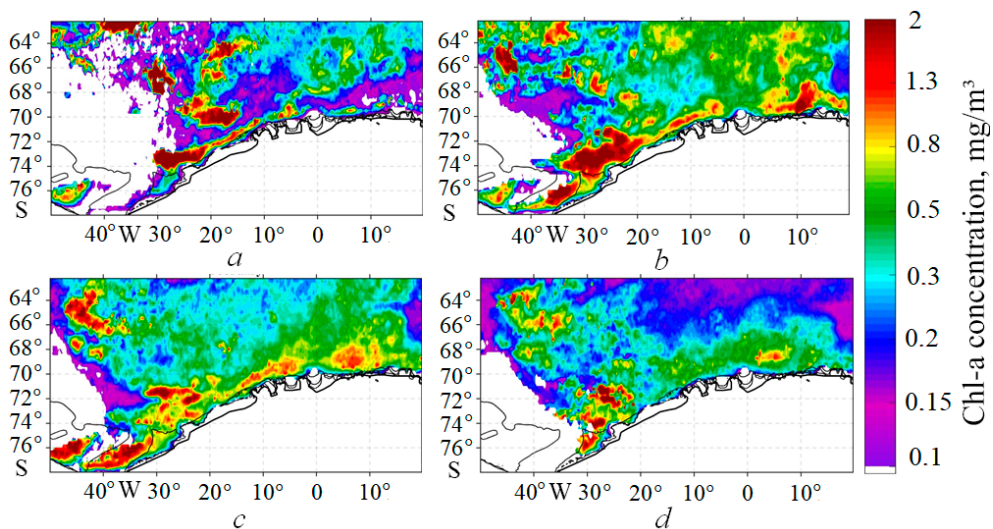


Fig. 14. Distribution of the monthly average Chl-a concentration in December (*a*), January (*b*), February (*c*) and March (*d*) in 2002–2019. The 100, 200 and 500 m isobaths are plotted on the maps

5. Conclusion

In this work, based on the analysis of MODIS Aqua satellite measurements for 2002–2019, for the first time, a study of the spatiotemporal variability of the seasonal Chl-a concentration variability in various regions of the South Atlantic and the Atlantic sector of the Southern Ocean was carried out. In general, over the entire area considered, there is a later start of blooming with a peak in Chl-a concentration as latitude increases. In the northern part, the Chl-a concentration peak is observed in November – December, and in the southern part, in January –

February, which is associated with the beginning of seasonal heating and the appearance of stable thermal stratification. However, in a number of regions this dependence is violated. In these areas, located to the east of powerful sources of nutrients (islands, shelf waters), the time to reach the peak values of Chl-a concentration is associated with the influence of phytoplankton and nutrients advection and occurs with a delay necessary for the transfer of impurities under the ACC influence.

Based on the analysis results in the selected region, four zones of local Chl-a concentration maxima were identified, namely: the Argentinean shelf; the South Georgia Islands; a part in the area of the Antarctic Peninsula water removal; the Antarctic shelf east of the Weddell Sea. A detailed analysis of the seasonal variability of the Chl-a concentration in the indicated zones was carried out. As a rule, the seasonal variability is associated with the location of certain features: islands, shelf and frontal zones, terrigenous suspension removal from the Parana and Uruguay rivers, marginal ice zone and the Polar Front. The important role of the Argentinean shelf waters, transported under the Brazil Current action and affecting the Chl-a concentration variability at 40°–45°S latitudes throughout the South Atlantic should be emphasized. Other known important sources of nutrients are the South Georgia Islands and the Antarctic shelf. The blooming of the marginal zone of Antarctica is characterized by pronounced heterogeneity with maxima in the southeastern Weddell Sea and in the Lazarev Sea.

Based on the data obtained, it can be concluded that the main factor in the appearance of increased Chl-a concentration areas is the influence of topography features on the ACC fronts, which specifies both the dynamic balance of the entire flow and the supply of nutrients with terrigenous suspensions, largely determining the South Atlantic bioproductivity. In high latitudes, the Chl-a concentration variability is also significantly affected by the marginal ice melting.

The analysis of long-term data demonstrates intense interannual variability in the Chl-a concentration. Its amplitudes can reach very high values. It is important to note that satellite observations make it possible to study Chl-a variability only in the surface layer. At the same time, the Chl-a concentration distribution in the Southern Ocean is characterized by powerful deep maxima, whose dynamics may differ from the dynamics of the maximum values of the surface Chl-a concentration.

In our following works, we are planning to study the features of the vertical distribution of the Chl-a concentration based on the new available array of measurements from Bio-Argo buoys and its interannual variability under the influence of various physical factors (cooling, ice cover and current regime).

REFERENCES

1. Banse, K., 1996. Low Seasonality of Low Concentrations of Surface Chlorophyll in the Subantarctic Water Ring: Underwater Irradiance, Iron, or Grazing? *Progress in Oceanography*, 37(3-4), pp. 241-291. doi:10.1016/S0079-6611(96)00006-7
2. Bowie, A.R., van der Merve, P., Quéroué, F., Trull, T., Fourquez, M., Planchon, F., Sarthou, G., Chever, F., Townsend, A.T. [et al.], 2015. Iron Budgets for Three Distinct Biogeochemical Sites around the Kerguelen Archipelago (Southern Ocean) during the Natural Fertilisation Study, KEOPS-2. *Bioesciences*, 12(14), pp. 4421-4445. doi:10.5194/bg-12-4421-2015

3. Vives, C.R., Schallenberg, C., Strutton, P.G. and Westwood, K.J., 2022. Iron and Light Limitation of Phytoplankton Growth off East Antarctica. *Journal of Marine Systems*, 234, 103774. doi:10.1016/j.jmarsys.2022.103774
4. Thomalla, S.J., Fauchereau, N., Swart, S. and Monteiro, P.M.S., 2011. Regional Scale Characteristics of the Seasonal Cycle of Chlorophyll in the Southern Ocean. *Biogeosciences*, 8(10), pp. 2849-2866. doi:10.5194/bg-8-2849-2011
5. Deppeler, S.L. and Davidson, A.T., 2017. Southern Ocean Phytoplankton in a Changing Climate. *Frontiers in Marine Science*, 4, 40. doi:10.3389/fmars.2017.00040
6. Sullivan, C.W., McClain, C.R., Comiso, J.C. and Smith Jr., W.O., 1988. Phytoplankton Standing Crops within an Antarctic Ice Edge Assessed by Satellite Remote Sensing. *Journal of Geophysical Research: Oceans*, 93(C10), pp. 12487-12498. doi:10.1029/JC093iC10p12487
7. Moore, J.K. and Abbott, M.R., 2002. Surface Chlorophyll Concentrations in Relation to the Antarctic Polar Front: Seasonal and Spatial Patterns from Satellite Observations. *Journal of Marine Systems*, 37(1-3), pp. 69-86. doi:10.1016/S0924-7963(02)00196-3
8. Sokolov, S. and Rintoul, S.R., 2007. On the Relationship between Fronts of the Antarctic Circumpolar Current and Surface Chlorophyll Concentrations in the Southern Ocean. *Journal of Geophysical Research: Oceans*, 112(C7), C07030. doi:10.1029/2006JC004072
9. Demidov, A.B., Vedernikov, V.I. and Sheberstov, S.V., 2007. Spatiotemporal Variability of Chlorophyll A in the Atlantic and Indian Sectors of the Southern Ocean during February-April of 2000 According to Satellite and Expeditionary Data. *Oceanology*, 47(4), pp. 507-518. doi:10.1134/S000143700704008X
10. Sallée, J.-B., Llort, J., Tagliabue, A. and Lévy, M., 2015. Characterization of Distinct Bloom Phenology Regimes in the Southern Ocean. *ICES Journal of Marine Science*, 72(6), pp. 1985-1998. doi:10.1093/icesjms/fsv069
11. Demidov, A.B., Gagarin, V.I. and Grigoriev, A.V., 2010. Seasonal Variability of the Surface Chlorophyll "A" in the Drake Passage. *Oceanology*, 50(3), pp. 327-341. doi:10.1134/S0001437010030045
12. Arrigo, K.R. and Van Dijken, G.L., 2003. Phytoplankton Dynamics within 37 Antarctic Coastal Polynya Systems. *Journal of Geophysical Research: Oceans*, 108(C8), 3271. doi:10.1029/2002JC001739
13. Arrigo, K.R., Van Dijken, G.L. and Bushinsky, S., 2008. Primary Production in the Southern Ocean, 1997–2006. *Journal of Geophysical Research: Oceans*, 113(C8), C08004. doi:10.1029/2007JC004551
14. Prend, C.J., Gille, S.T., Talley, L.D., Mitchell, B.G., Rosso, I. and Mazloff, M.R., 2019. Physical Drivers of Phytoplankton Bloom Initiation in the Southern Ocean's Scotia Sea. *Journal of Geophysical Research: Oceans*, 124(8), pp. 5811-5826. doi:10.1029/2019JC015162
15. Demidov, A.B., Mosharov, S.A. and Gagarin, V.I., 2012. Meridional Asymmetric Distribution of the Primary Production in the Atlantic Sector of the Southern Ocean in the Austral Spring and Summer. *Oceanology*, 52(5), pp. 623-634. doi:10.1134/S0001437012050050
16. Artamonov, Yu.V. and Skripaleva, E.A., 2016. Oceanographic Research of Marine Hydrophysical Institute in the Southern Ocean. *Physical Oceanography*, (6), pp. 56-66. doi:10.22449/1573-160X-2016-6-56-66
17. Artamonov, Y.V., Skripaleva, E.A., Shutov, S.A. and Artamonov, A.Y., 2020. Thermohaline Structure of Water in Antarctic Coastal Areas in March-April 2019 Derived from the 64th Russian Antarctic Expedition Measurements. *Russian Meteorology and Hydrology*, 45(2), pp. 87-95. doi:10.3103/S1068373920020041
18. Morozov, E.G., Spiridonov, V.A., Molodtsova, T.N., Frey, D.I., Demidova, T.A. and Flint, M.V., 2020. Investigations of the Ecosystem in the Atlantic Sector of Antarctica (Cruise 79 of the R/V Akademik Mstislav Keldysh). *Oceanology*, 60(5), pp. 721-723. doi:10.1134/S0001437020050161

19. Vereshchaka, A.L., Lunina, A.A. and Mikaelyan, A.S., 2022. Surface Chlorophyll Concentration as a Mesoplankton Biomass Assessment Tool in the Southern Ocean Region. *Global Ecology and Biogeography*, 31(3), pp. 405-424. doi:10.1111/geb.13435
20. O'Reilly, J.E. and Werdell, P.J., 2019. Chlorophyll Algorithms for Ocean Color Sensors – OC4, OC5 & OC6. *Remote Sensing of Environment*, 229, pp. 32-47. doi:10.1016/j.rse.2019.04.021
21. Garcia, C.A.E., Tavano Garcia, V.M. and McClain, C.R., 2005. Evaluation of SeaWiFS Chlorophyll Algorithms in the Southwestern Atlantic and Southern Oceans. *Remote Sensing of Environment*, 95(1), pp. 125-137. doi:10.1016/J.RSE.2004.12.006
22. Brewin, R.J., Raitos, D.E., Dall'Olmo, G., Zarokanellos, N., Jackson, T., Racault, M.-F., Boss, E.S., Sathyendranath, S., Jones, B.H., [et al.], 2015. Regional Ocean-Colour Chlorophyll Algorithms for the Red Sea. *Remote Sensing of Environment*, 165, pp. 64-85. doi:10.1016/j.rse.2015.04.024
23. Cai, Y., Chen, D., Mazloff, M.R., Lian, T. and Liu, X., 2022. Topographic Modulation of the Wind Stress Impact on Eddy Activity in the Southern Ocean. *Geophysical Research Letters*, 49(13), e2022GL097859. doi:10.1029/2022GL097859

About the authors:

Arseniy A. Kubryakov, Senior Research Associate, Marine Hydrophysical Institute of RAS (2 Kapitanskaya Str., Sevastopol, 299011, Russian Federation), Ph.D. (Phys.-Math), **ORCID ID: 0000-0003-3561-5913**, arskubr@mhi-ras.ru

Elena A. Kubryakova, Senior Research Associate, Marine Hydrophysical Institute of RAS (2 Kapitanskaya Str., Sevastopol, 299011, Russian Federation), Ph.D. (Phys.-Math), **ORCID ID: 0000-0001-6071-1881**, elena.kubryakova@mhi-ras.ru

Yana I. Bakueva, Junior Research Associate, Marine Hydrophysical Institute of RAS (2 Kapitanskaya Str., Sevastopol, 299011, Russian Federation), ybakueva@mhi-ras.ru

Contribution of the co-authors:

Arseniy A. Kubryakov – conceptualization, preparation of the paper text

Elena A. Kubryakova – data analysis, formulation of results and preparation of the final version of the paper text

Yana I. Bakueva – visualization, numerical calculations, preparation of the paper text

The authors have read and approved the final manuscript.

The authors declare that they have no conflict of interest.